Supporting Information

Unexpected sequence adsorption features of polynucleotide ssDNA on graphene oxide

Huishu Ma[a,b], Zhen Xu[c], Haiping Fang[d,e], Xiaoling Lei[d,e*]

[a] *Division of Interfacial Water and Key Laboratory of Interfacial Physics and Technology, Shanghai Institute of Applied Physics, Chinese Academy of Sciences, P.O. Box 800-204, Shanghai, 201800, China*

[b] *University of Chinese Academy of Sciences, Beijing, 100049, China*

[c] *College of Mechanical Engineering, Shanghai University of Engineering Science, Shanghai, 201620, China*

[d] *Department of Physics, East China University of Science and Technology, Shanghai 200237, China*

[e] *Zhangjiang Laboratory, Shanghai Advanced Research Institute, Chinese Academy of Sciences, Shanghai 201210, China*

Contents

S1. Initial conformations for simulation with polynucleotide ssDNA molecule and with single nucleotides

The GO nanosheet was constructed based on the Shi-Tu structure model[1] with the formula of $C_{10}O_1(OH)_1(COOH)_{0.5}$[2-4]. The size of the GO nanosheet was 10.084 nm × 10.224 nm in the *xz* plane (Fig. S1(a)), which contained 3936 carbon atoms, 311 hydroxyl groups (-OH) and 290 epoxy groups (-O-). The distribution of functional/oxidized groups on GO nanosheet was generated according to the rate-constant ratios based on the computation of both density functional theory and conventional transition-state theory. The oxidation loci on GO was highly correlated, in accordance with the experimental observations[5-12], recently. This high correlation led to the coexistence of both large unoxidized and oxidized regions on GO nanosheet. The correlation length was 4.2±0.5 nm in our GO model. More importantly, on the oxidized regions of GO nanosheet, there were also some small areas of sp2-hybridized domains that we called 'island' region. Based on the correlations, the size of the patch islands was estimate to be up to 0.65±0.03 nm.

In this paper, based on the molecular dynamics (MD) simulation, we systematically study the sequence features of polynucleotide ssDNA molecules adsorption on GO surface in aqueous solutions. As shown in Fig. S1(b) and (c), two series of systems have been studied to illustrate the adsorption behavior of ssDNA on GO surface, among which were the single nucleotide (A, C, G and T) and polynucleotide ssDNA molecules (A_{12}, C_{12}, G_{12} and T_{12}). For the single nucleotide system, ten nucleotides were random placed above the GO surface with the centroid distance of 1.5 nm at the beginning of the simulation and then each system was run for 100 ns. For the polynucleotide system, the ssDNA molecule was random placed at least 0.5 nm away from the GO surface at the beginning of the simulation and then each sample was run for 400 ns.

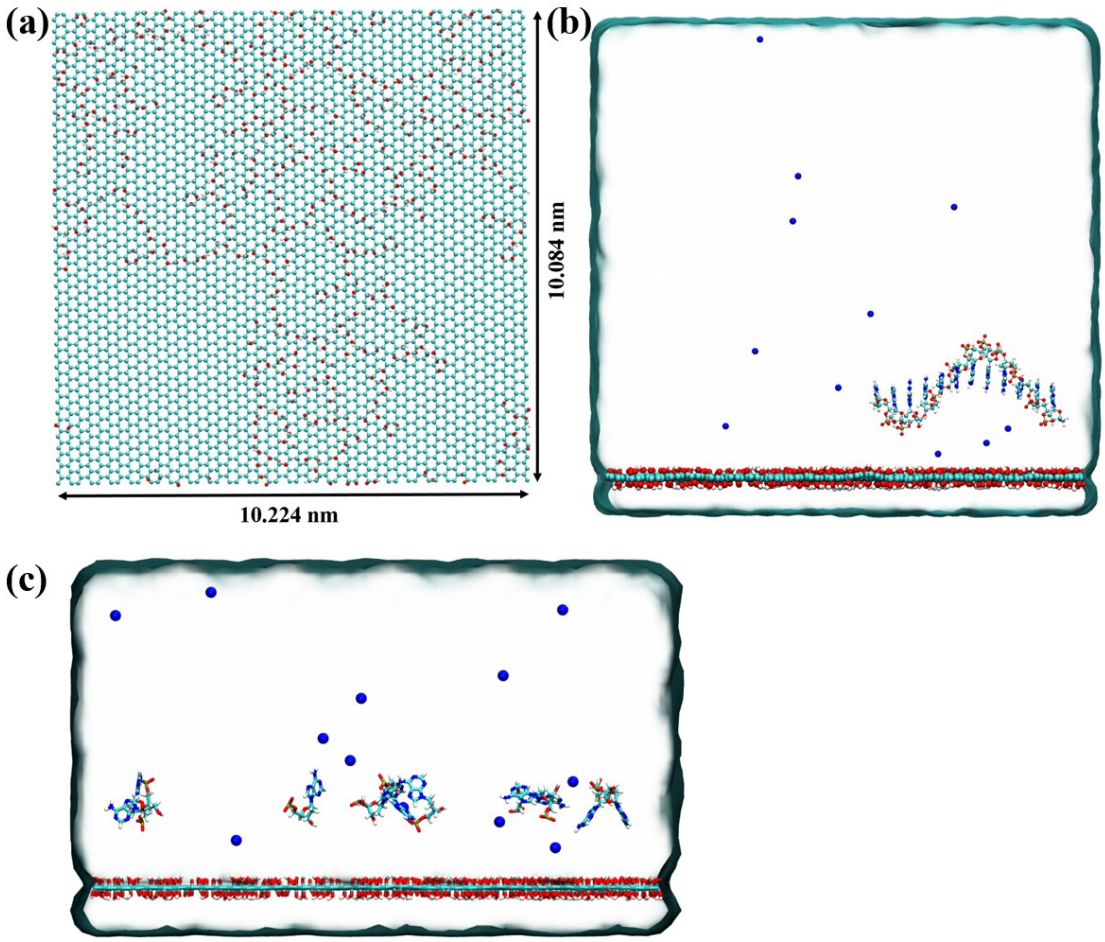

Fig. S1 (a) Snapshot (top view) of the model GO sheet. C, O and H atoms were represented by the cyan, red and white spheres correspondingly. (b) Snapshot (side view) of the simulation system with polynucleotide ssDNA molecule at initial time. (c) Snapshot (side view) of the system with single nucleotides. Na atoms were represented by the blue sphere.

S2. Adsorption conformations of polynucleotide ssDNAs

We presented the final adsorption conformations of polynucleotide ssDNAs (A_{12}, C_{12}, G_{12} and T_{12}) on GO surface. As shown in Fig. S2, all the ssDNA segments were fully or partly adsorbed on the oxidized region, which was consistent with our previous research that the ssDNA segment shows preferential binding to oxidized regions compared to unoxidized regions of the GO surface[13]. Even for the same sequences of ssDNA molecules, the final conformations of adsorbed ssDNA molecules differed from each simulation samples, including extended and coiled conformations. For A_{12}, C_{12} and T_{12}, most of the samples showed extended conformations. However, for G_{12}, it mainly coiled adsorbed on GO surface, only two

samples showing extended conformations. It meant G_{12} produced a coiled structure on GO surface. As we known, poly G is a synthetically and experimentally challenging homopolymer because of its folding and self-aggregation[14, 15]. Our simulation results were also consistent with this conformation character.

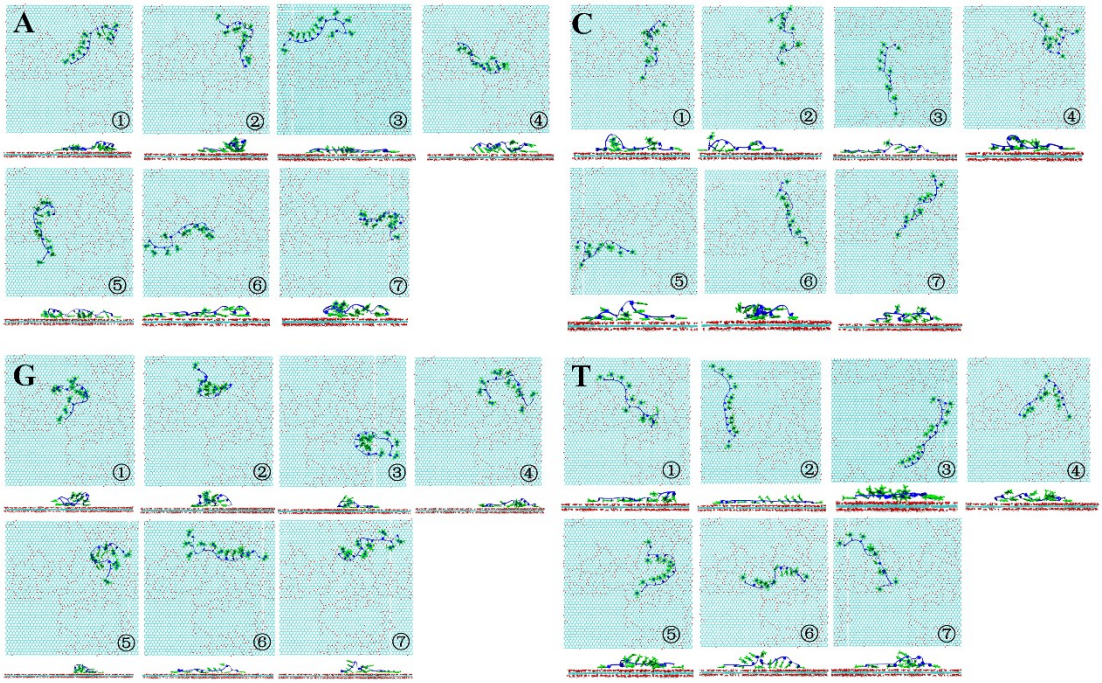

Fig. S2 Snapshots (both top and side views) of the final adsorption conformation of polynucleotide ssDNAs (A_{12}, C_{12}, G_{12} and T_{12}) on GO surface.

S3. RMSD for polynucleotide ssDNAs and atom number of contacts between GO surface and the four ssDNAs

In order to show the convergence of simulation system, we calculated the root mean square displacement (RMSD) of ssDNAs and atom number of contacts (N) between GO surface and four ssDNAs employed in this study.

Stability of the final adsorption geometries can be judged on the RMSD of the ssDNA (Fig. S3(a)), which became saturated except for some fluctuation in the last 50 ns for all simulations and showing their convergence after 200 ns.

The atom number of contacts between GO surface and the adsorbing ssDNA reflects the ssDNA adsorption affinity. For analysis, a contact between ssDNA and GO is considered if any of the ssDNA atoms is within a cutoff distance of 1.2 nm to

$$N_c(t) = \sum_{i=1}^{N_{GO}} \sum_{j=1}^{N_{ssDNA}} \int_{r_i}^{r_i + 1.2nm} \delta[r(t) - r_j(t)]dr$$

the GO surface and is calculated as . As shown in Fig. S3(b), the A_{12}, C_{12}, G_{12}, and T_{12} adsorptions had something in common. Initially, N was zero when the ssDNA was not absorbed on the GO surface. After a few nanoseconds, the ssDNA made the first contact via π–π stacking of a nucleobase. Then, N increased sharply and concurrently in a stepwise fashion, as different segments of the ssDNA sequentially absorbed onto the surface and increase interactions with the GO. In all of the simulations, N eventually fluctuated around a stable value, indicating that the hybrid system attained a stable conformation.

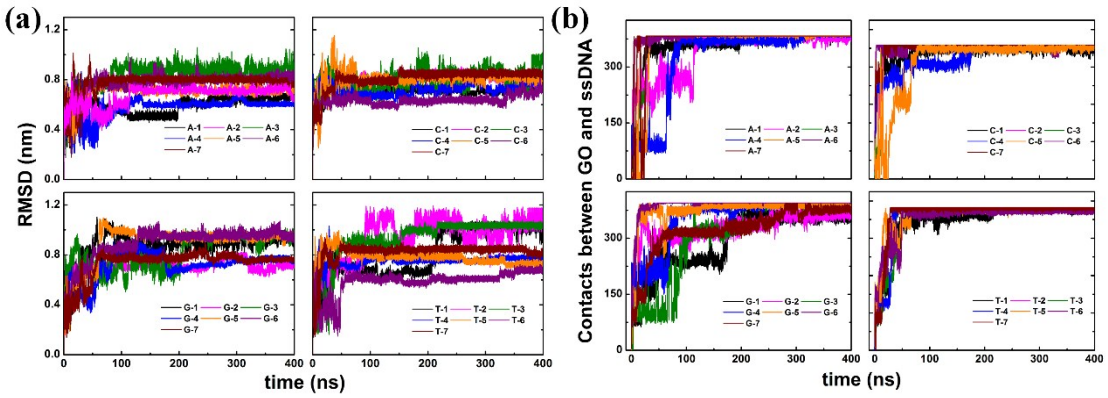

Fig. S3 Time evolution of (a) the RMSD of ssDNAs and (b) atom number of contacts (N) between GO surface and the four ssDNAs employed in this study for the entire trajectories of the 400 ns production simulations.

S4. Dynamic adsorption of polynucleotide ssDNAs onto GO surface

To show the dynamic adsorption of polynucleotide ssDNAs with different sequences onto GO surface, we calculated the interaction energy between GO surface and ssDNA molecules with different sequences as shown in Fig. S4(a). Initially, ssDNA was placed above the GO surface, and they were completely noninteracting. However, as the simulations started, the interaction energy first undergoes some initial fluctuation, representing solvent-assisted free diffusion of the ssDNA. Thereafter, the interaction energy gradually reduced and attained constancy, indicating the stepwise adsorption of ssDNA molecules onto GO surface. In the last 50 ns of the simulation, the interaction energy fluctuated steadily, suggesting that the adsorption of ssDNA was in a dynamic equilibrium state.

Then, to further explore the sequence feature of ssDNA molecules on GO surface, the radius of gyration (R_g) for every simulation sample was calculated. As shown in Fig. S4(b), R_g oscillated up or down from 1.3 nm of the initial conformation to reach a stable value with a maximum of 2.0 nm and a minimum of 0.9 nm. Moreover, different ssDNA molecules with different sequences show different characteristics, which were described in our Manuscript.

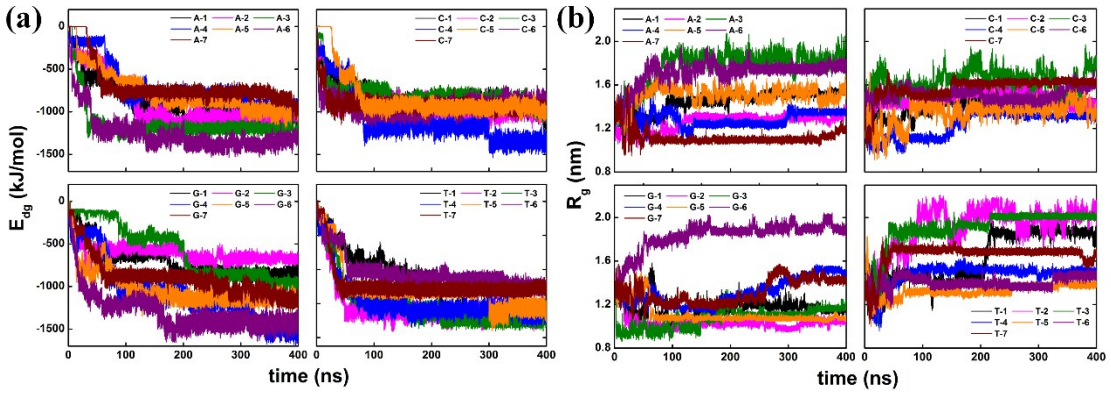

Fig. S4 Time evolution of (a) interaction energy between GO surface and ssDNAs and (b) radius of gyration (R_g) for the four kinds of polynucleotide ssDNAs considered in this study. Results from independent molecular dynamics (MD) samples were represented by different colors.

S5. Dynamic adsorption of single nucleotides (A, C, G and T) onto GO surface

We calculated the interaction energy between GO and A, C, G, T nucleotides and found that the interaction energy differed in the system composed of not only same kind of nucleotide but also different kind of nucleotide, as shown in Fig. S5(a). Further analysis showed that each nucleotide could be adsorbed on either the oxidized or the unoxidized region on the GO. Fig. S5(b) shows the average interaction energy between GO surface and nucleotides A, C, G and T at last 20 ns. It suggested that different adsorption site could result to the distinguishable interaction energy between nucleotide and GO, even for the same kind of nucleotide. Fig. S5(c) shows the centroid displacement fluctuations in last 20 ns after the nucleotides adsorption in oxidized and unoxidized regions. In unoxidized region, the fluctuation was larger than in oxidized region, which meant that single nucleotide also could slip in oxidized region, but the slip area is much smaller than unoxidized region because of the steric hindrance of the hydroxy and epoxy groups on the basal plane of the GO sheet. It is obvious that single nucleotides could slip on the GO surface after their stably

adsorption on GO surface.

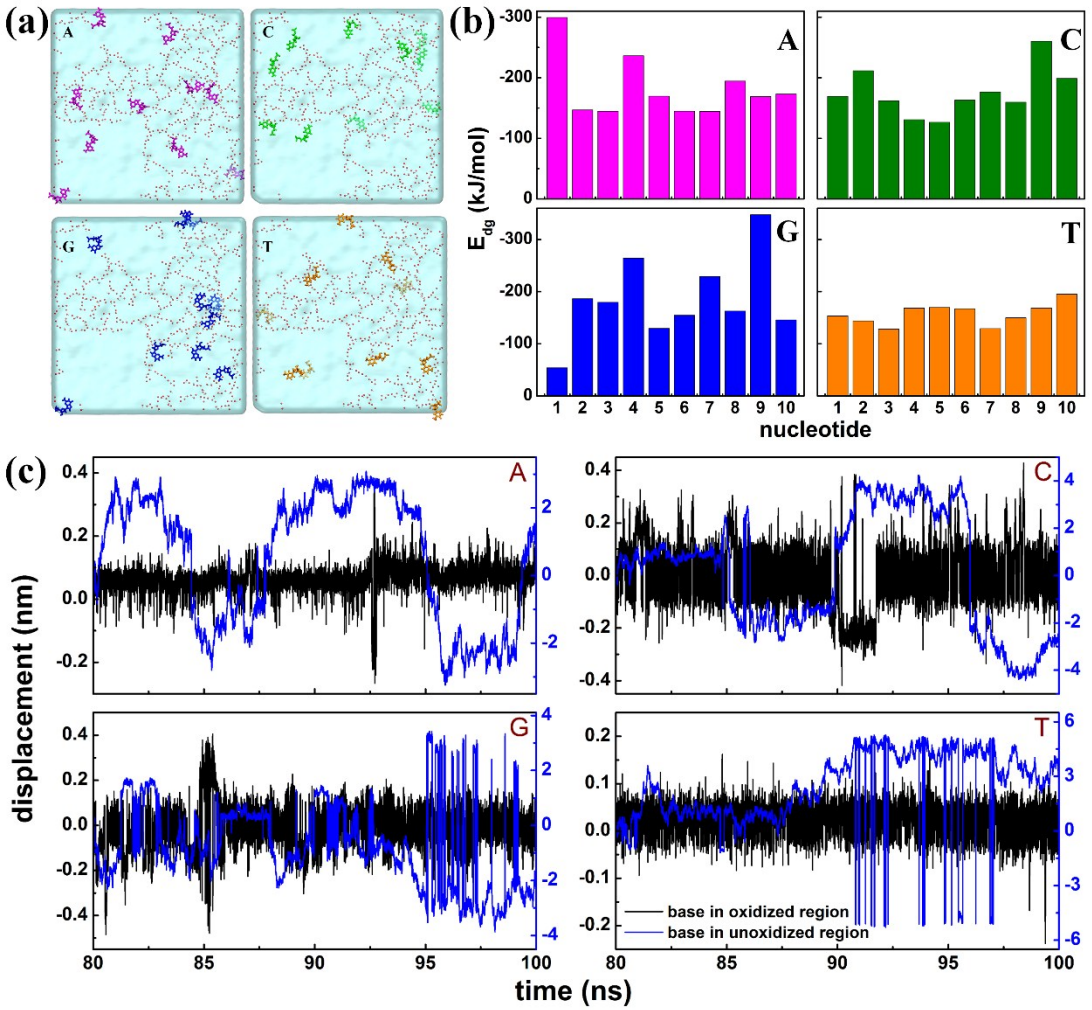

Fig. S5 (a) Snapshots (top view) of nucleotides-GO hybrids for nucleotides A, C, G, T at final simulation time. (b) Average interaction energy between all nucleotides and GO surface at last 20 ns in simulation systems for nucleotide A, C, G, T. (c) Time evolution displacement of centroid (d) from t_0 (t_0=80 ns) to t_1 for the nucleobase A, C, G, T when adsorbed on the corresponding oxidized region (black line) and unoxidized region (blue line) of GO surface.

S6. Hydrogen bonds between polynucleotide ssDNAs and GO surface

Due to the thermal perturbation of water molecules, the fluctuation of the hydrogen bonds number was large. To illustrate the changes of hydrogen bonds number as a function of time more clearly, we averaged the number of hydrogen bonds in every 2 ns during the whole 400 ns. As we known, the GO nanosheet in our simulation contained 311 hydroxyl groups (-OH) and 290 epoxy groups (-O-), giving the number radio between them is nearly 1. However, as shown in Fig. S6, the hydrogen bonds formed between polynucleotide ssDNAs (A_{12}, C_{12}, G_{12} and T_{12}) and hydroxyl group were much more than that formed between the same ssDNA molecule and epoxy

group during the adsorption process, indicating that hydroxyl groups were more likely to interact with the GO surface than the epoxy groups.

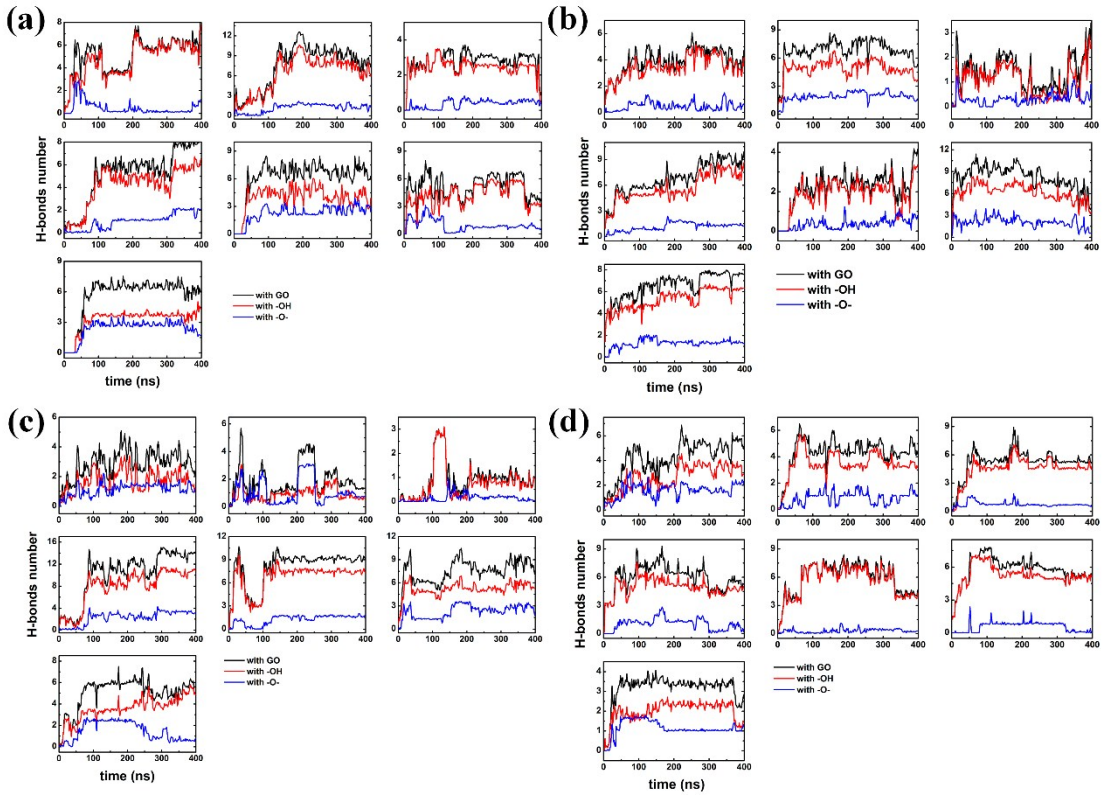

Fig. S6 Number of hydrogen bonds between the polynucleotide ssDNAs (a) A_{12}, (b) C_{12}, (c) G_{12} and (d) T_{12} and the GO surface: the total number of hydrogen bonds (black line), the number of hydrogen bonds formed with the hydroxyl groups (red line), the number of hydrogen bonds formed with the epoxy groups (blue line).

We also calculated the average number of hydrogen bonds between polynucleotide ssDNAs (A_{12}, C_{12}, G_{12} and T_{12}) and GO at last 20 ns, as shown in Fig. S7. From the result, we found that all polynucleotide ssDNA molecules could form more hydrogen bonds with the hydroxyl groups on the GO than that with the epoxy groups, which was in accordance with our precious results of the 12 mer ssDNA with random sequences on GO[13].

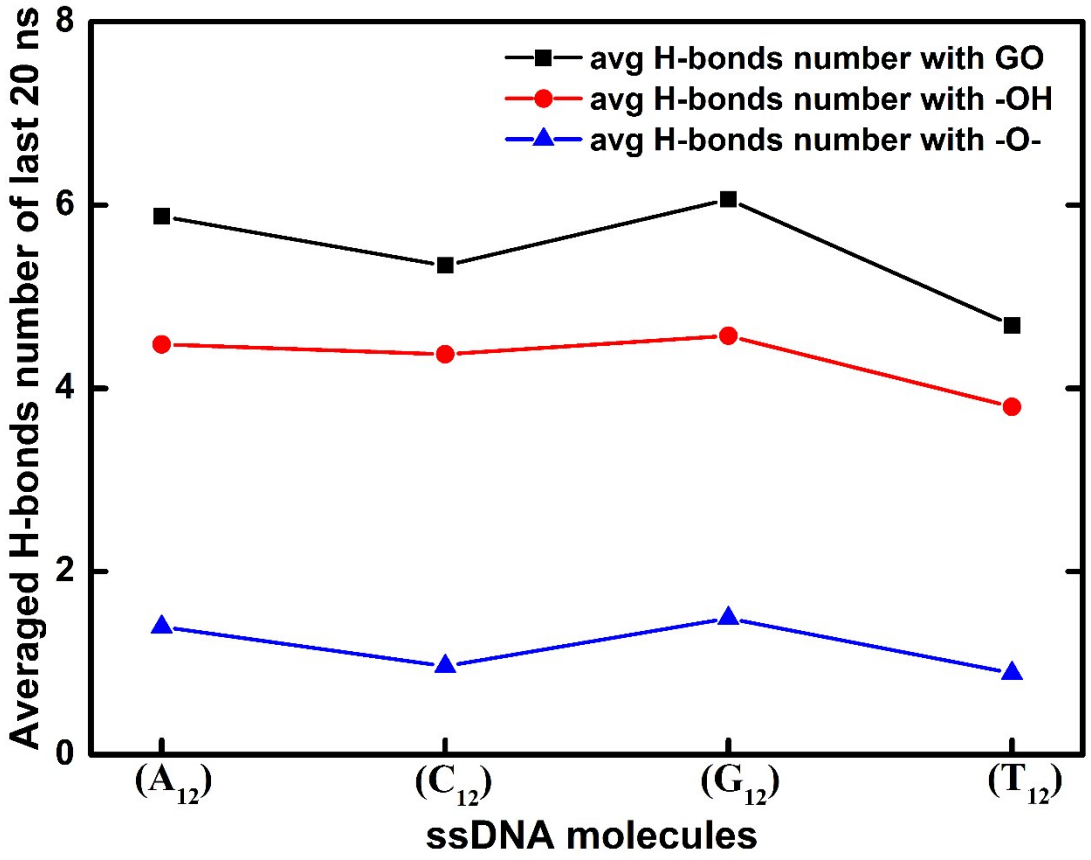

Fig. S7 Average number of hydrogen bonds formed between polynucleotide ssDNA molecules (A_{12}, C_{12}, G_{12} and T_{12}) and GO (black), hydroxyl groups (red) and epoxy groups (blue) at last 20 ns.

1. J. Yang, G. Shi, Y. Tu and H. Fang, *Angewandte Chemie International Edition*, 2014, **53**, 10190-10194.
2. A. Lerf, H. He, M. Forster and J. Klinowski, *The Journal of Physical Chemistry B*, 1998, **102**, 4477-4482.
3. N. V. Medhekar, A. Ramasubramaniam, R. S. Ruoff and V. B. Shenoy, *ACS nano*, 2010, **4**, 2300-2306.
4. C.-J. Shih, S. Lin, R. Sharma, M. S. Strano and D. Blankschtein, *Langmuir*, 2011, **28**, 235-241.
5. Y. Tu, M. Lv, P. Xiu, T. Huynh, M. Zhang, M. Castelli, Z. Liu, Q. Huang, C. Fan and H. Fang, *Nature nanotechnology*, 2013, **8**, 594.
6. H. Geng, X. Liu, G. Shi, G. Bai, J. Ma, J. Chen, Z. Wu, Y. Song, H. Fang and J. Wang, *Angewandte Chemie International Edition*, 2017, **56**, 997-1001.
7. D. Chen, H. Feng and J. Li, *Chemical reviews*, 2012, **112**, 6027-6053.
8. D. R. Dreyer, S. Park, C. W. Bielawski and R. S. Ruoff, *Chemical society reviews*, 2010, **39**, 228-240.
9. W. Cai, R. D. Piner, F. J. Stadermann, S. Park, M. A. Shaibat, Y. Ishii, D. Yang, A. Velamakanni, S. J. An and M. Stoller, *Science*, 2008, **321**, 1815-1817.
10. J. C. Meyer, C. O. Girit, M. Crommie and A. Zettl, *Nature*, 2008, **454**, 319.

11. K. A. Mkhoyan, A. W. Contryman, J. Silcox, D. A. Stewart, G. Eda, C. Mattevi, S. Miller and M. Chhowalla, *Nano letters*, 2009, **9**, 1058-1063.
12. K. Erickson, R. Erni, Z. Lee, N. Alem, W. Gannett and A. Zettl, *Advanced Materials*, 2010, **22**, 4467-4472.
13. Z. Xu, X. Lei, Y. Tu, Z. J. Tan, B. Song and H. Fang, *Chemistry–A European Journal*, 2017, **23**, 13100-13104.
14. Y. X. Wang, *J. Phys. Chem. C*, 2008, **112**, 14297-14305.
15. H. Sigel, *Biol. Trace Elem. Res.*, 1989, **21**, 49-59.